Deficiency in Phylloquinone (Vitamin K₁) Methylation Affects Prenyl Quinone Distribution, Photosystem I Abundance, and Anthocyanin Accumulation in the *Arabidopsis AtmenG* Mutant*

Antje Lohmann[‡], **Mark Aurel Schöttler**[§], **Claire Bréhélin**[¶1], **Felix Kessler**[¶1], **Ralph Bock**[§], **Edgar B. Cahoon**[||], **and Peter Dörmann**[‡2]

From the Departments of ‡Molecular Physiology, and §Organelle Biology, Biotechnology, and Molecular Ecophysiology, Max Planck Institute of Molecular Plant Physiology, Am Mühlenberg 1, 14476 Potsdam, Germany, the ¶Laboratory of Plant Biology, Institute of Biology, University of Neuchâtel, rue Emile Argand 11, CP 158, CH-2009 Neuchâtel, Switzerland, and the ||USDA-Agricultural Research Service Plant Genetics Research Unit, Donald Danforth Plant Science Center, St. Louis, Missouri 63132

Phylloquinone (vitamin K₁) is synthesized in cyanobacteria and in chloroplasts of plants, where it serves as electron carrier of photosystem I. The last step of phylloquinone synthesis in cyanobacteria is the methylation of 2-phytyl-1,4-naphthoquinone by the *menG* gene product. Here, we report that the uncharacterized *Arabidopsis* gene At1g23360, which shows sequence similarity to *menG*, functionally complements the *Synechocystis menG* mutant. An *Arabidopsis* mutant, *AtmenG*, carrying a T-DNA insertion in the gene At1g23360 is devoid of phylloquinone, but contains an increased amount of 2-phytyl-1,4-naphthoquinone. Phylloquinone and 2-phytyl-1,4-naphthoquinone in thylakoid membranes of wild type and *AtmenG*, respectively, predominantly localize to photosystem I, whereas excess amounts of prenyl quinones are stored in plastoglobules. Photosystem I reaction centers are decreased in *AtmenG* plants under high light, as revealed by immunoblot and spectroscopic measurements. Anthocyanin accumulation and chalcone synthase (CHS1) transcription are affected during high light exposure, indicating that alterations in photosynthesis in *AtmenG* affect gene expression in the nucleus. Photosystem II quantum yield is decreased under high light. Therefore, the loss of phylloquinone methylation affects photosystem I stability or turnover, and the limitation in functional photosystem I complexes results in overreduction of photosystem II under high light.

In plants and cyanobacteria, photosynthetic conversion of light into chemical energy is mediated via two photosystems, photosystem I (PSI)[3] and photosystem II (PSII). PSII transfers electrons from water onto plastoquinone, an abundant prenyl quinone in thylakoids. PSI accepts electrons from plastocyanin, and they are subsequently transferred onto ferredoxin or flavodoxin. PSI forms dimers in thylakoids, with each PSI monomer harboring a special chlorophyll *a* pair (reaction center P₇₀₀) for charge separation. The electron transfer chain through one PSI monomer encompasses two branches, each containing two further chlorophyll *a* molecules (A and A₀) and one phylloquinone (A₁). Electron flux merges at the iron-sulfur center F_X, which passes electrons on to the iron-sulfur centers F_B and F_A (1–3). The two branches of the PSI electron transfer chain are not structurally equivalent and differ in their lipid association: Whereas phosphatidylglycerol is found in close proximity to one of the branches, monogalactosyldiacylglycerol is associated with the other branch (2). It is presently unclear whether these branches are active to similar extents (4, 5).

Phylloquinone (vitamin K₁) is an essential component of the human diet, because it serves as a cofactor for γ-carboxylation of glutamyl residues in different proteins, such as blood coagulation factors, but cannot be synthesized in animals and humans (6). The phylloquinone molecule is composed of a naphthoquinone ring, which can exist in the oxidized quinone or in the reduced hydroquinone form, and a prenyl side chain derived from phytyl-diphosphate. The biosynthesis of menaquinone, a bacterial vitamin K analog carrying an unsaturated side chain, and of phylloquinone has been studied in *Escherichia coli* and in cyanobacteria, respectively (7–9). The naphthoquinone ring is derived from chorismate, which is converted into 1,4-dihydroxy-2-naphthoate (DHNA) by six consecutive reactions (Fig. 1). Subsequently, DHNA is converted to 2-phytyl-1,4-naphthoquinone (PNQ) by DHNA phytyltransferase (MenA). The last step of phylloquinone synthesis in cyanobacteria involves the methylation at the C3-position of the naphthoquinone moiety by the *menG* gene product, thereby converting the unmethylated form, 2-phytyl-1,4-naphthoquinone, into phylloquinone.

The role of phylloquinone in photosynthesis has been studied by employing loss-of-function mutants of cyanobacteria

quinone; PSII, photosystem II; DHNA, 1,4-dihydroxy-2-naphthoate; MES, 4-morpholineethanesulfonic acid; WT, wild type; Cyt, cytochrome.

(*menA*, *menB*, *menD*, *menE*, *menG*) (7, 9, 10). A block in biosynthesis resulting in total loss of phylloquinone has only a minor impact on photosynthesis or growth of *Synechocystis* under low light conditions, presumably, because other hydroquinones, such as plastoquinone, can largely substitute for phylloquinone deficiency in PSI (7). However, under high light conditions, photoautotrophic growth of *Synechocystis menA* and *menB* mutant strains is severely compromised (7).

Phylloquinone synthesis in plants has been studied by feeding biosynthetic precursors and by enzyme assays in spinach, *Capsicum annuum*, *Euglena gracilis*, and *Galium* cell cultures (11–14). The first genetic study of phylloquinone synthesis in plants was presented by the isolation of the *AtmenA* mutant of *Arabidopsis* carrying a block in DHNA phytyltransferase. *AtmenA* plants are totally devoid of phylloquinone, contain reduced amounts of chlorophyll and PSI and show a severe reduction in photosynthetic efficiency (15). As a consequence, mutant plants are unable to survive in soil, providing strong evidence for the importance of phylloquinone as essential electron carrier of PSI (15). Furthermore, the gene and corresponding mutant of a multifunctional protein carrying four enzymatic domains putatively involved in phylloquinone synthesis (MenF, MenD, MenC, lipase) were recently isolated from *Arabidopsis* (16).

Disruption of the *menG* gene encoding PNQ methyltransferase resulted in phylloquinone deficiency in *Synechocystis* (10). In their PSI particles, mutant cells contained two molecules of 2-phytyl-1,4-naphthoquinone, the substrate of the MenG reaction, per PSI monomer. The gene encoding PNQ methyltransferase has not been isolated from higher plants, and the role of the final methylation reaction in phylloquinone synthesis for functional integrity of PSI in plants has not been studied. For this reason, the cDNA for an open reading frame identified as potentially homologous to *menG* and found in the fully sequenced genome of *Arabidopsis*, At1g23360, was isolated and its gene product tested for PNQ methyltransferase activity by expression in a heterologous system. The subplastidial distribution of phylloquinone and of PNQ was measured in *Arabidopsis* wild type and in an *AtmenG* knock-out mutant. Furthermore, biochemical and physiological characterization of the *AtmenG* mutant demonstrated that the 3-methyl group of phylloquinone is required to sustain maximal efficiency of photosynthetic electron transport, particularly at high light conditions.

MATERIALS AND METHODS

Isolation of the At1g23360 cDNA and Complementation of the Synechocystis menG Mutant—A cDNA corresponding to the *Arabidopsis* gene At1g23360 was isolated by PCR from an *Arabidopsis* (Columbia) cDNA library prepared from inflorescences, stems and leaves using the primers At1g23360-forward (5′-ATC TTA TA<u>C ATA TG</u>G CGG CTC TAC TCG GTA TCG) and At1g23360-reverse (5′-TAT <u>GGA TCC</u> TTT ACC TCA TAG CGA CCA AAT CC). The amplification product, which contained added flanking NdeI and BamHI restriction sites (underlined) was subcloned into the EcoRV site of pBluescriptIISK+ (Stratagene) to generate pBluescript-At1g23360. Sequencing revealed that this clone contains an authentic full-

length open reading frame derived from the locus At1g23360. A *Synechocystis menG* knock-out mutant was prepared by replacement of the sll1653 gene with a spectinomycin resistance marker through homologous recombination (17). A *menG*-specific knock-out vector was generated using procedures similar to those described previously (18). Initially, sequences flanking sll1653 were amplified from *Synechocystis* sp. PCC6803 genomic DNA. Primers used for amplification of a 541-base pair 5′-flanking sequence were: 5′-AAG TTT GGA TTG CGC CAG ATG-3′ (primer 5′-A) and 5′-GCT GTA CGC TCT CCT GAG TCG-3′ (primer 5′-B). Primers used for amplification of a 612-base pair 3′-flanking sequence were: 5′-GAC TCA GGA GAG CGT ACA <u>GCG TAC G</u>AC CGC TTT CCC ACT GGC C-3′ (primer 3′-A) and 5′-CCT AGC AGT GAC ACT TTC CGC C-3′ (primer 3′-B). The purified PCR products were combined and reamplified along with primers 5′-A and 3′-B to generate a contiguous sequence that contained an added BsiWI restriction site (underlined nucleotides in primer 3′-A) between the 5′- and 3′-flanking sequences. This product was cloned into the pGEM-T Easy vector (Promega) to generate the plasmid pMenG-KO. An *aadA* gene encoding a spectinomycin resistance marker was cloned into the BsiWI site of pMenG-KO to generate pMenG-Spec-KO. This plasmid was introduced into *Synechocystis* sp. PCC6803 as described (17), and homologous recombinant lines were selected for spectinomycin resistance. Replacement of the sll1653 gene with the spectinomycin resistance marker was confirmed by PCR analyses of genomic DNA. Complementation of the *Synechocystis menG* knock-out mutant was conducted by expression of the full-length *AtmenG* cDNA using the vector pSynExp-2 (18). The *AtmenG* cDNA was isolated as an NdeI/BamHI restriction fragment from pBluescript-At1g23360 and cloned into the NdeI/BglII sites of pSynExp-2 downstream of the *psbA2* promoter. The resulting plasmid was introduced into the *Synechocystis menG* knock-out mutant, and recombinant lines were selected by chloramphenicol and spectinomycin resistance. Incorporation of the *AtmenG* cDNA expression cassette was confirmed by PCR analyses of genomic DNA. Total lipids were extracted as previously described (18) from wild type (WT) cells, *menG* knock-out lines, and *AtmenG*-complemented knock-out lines that were maintained on solid BG11 medium (17) with appropriate antibiotic selection.

Phylloquinone Measurements—Phylloquinone was quantified according to Jakob and Elmadfa (20). Briefly, ca. 100 mg of leaf material was ground in liquid nitrogen. Lipids were extracted from leaves or cyanobacteria with 0.8 ml of isopropyl alcohol/hexane (3:1) after addition of menaquinone-4 as internal standard (250 ng in 50 μl of ethanol, Sigma). After vortexing, samples were centrifuged at 14,000 $\times$ g for 2 min, and the green lipid phase transferred to a new vial. The remaining pellet was again extracted with 0.6 ml of hexane. To the combined organic phases, 0.6 ml of methanol/water (9:1) was added, and after vortexing and centrifugation, the upper hexane phase transferred to a glass vial. The solvent was evaporated with nitrogen gas and the residue dissolved in 100 μl of methanol/dichloromethane (9:1). Phylloquinone was quantified on a 1100 Series HPLC (Agilent). Lipids were separated by isocratic chromatography (flow rate: 1 ml min^{-1}) on a reversed phase RP18

column (Eurosphos-100, 250 × 4.6 mm, Knauer, Germany) equipped with a post-column derivatization cartridge (30 × 4 mm, filled with Zink powder, 63-μm particle size, VWR) to reduce all quinones to their respective hydroquinone forms. The solvent was composed of 900 ml of methanol, 100 ml of dichloromethane, and 5 ml of a methanolic solution of 1.37 g of $ZnCl_2$, 0.41 g of sodium acetate, and 0.30 g of acetic acid. Phylloquinone was measured by fluorescence (excitation, 243 nm; emission, 430 nm) using menaquinone-4 as internal standard.

Subcellular Localization of the At1g23360 Protein—The entire open reading frame of the At1g23360 cDNA was amplified by PCR (primers: PD592, 5′-AGG GAT CCt ATG GCG GCT CTA CTC GGT A-3′; PD593, 5′-ATC CAT GGA CCT CAT AGC GAC CAA ATT C-3′) from pBluescript-At1g23360 (see above). The PCR fragment was ligated into the BamHI and NcoI sites of pCL60 (21) in translational fusion with the N terminus of the green fluorescent protein (GFP) sequence. Plasmid DNA was coated onto 1.0-μm gold microcarriers (Bio-Rad) and transferred into *Arabidopsis* leaves in a Biolistic PSD-1000/He particle delivery system (Bio-Rad) using 1100 psi rupture discs. After bombardment, leaves were incubated on Murashige and Skoog (22) medium in the dark for 2 days. Fluorescence signals were analyzed under a Leica DM-IRBE confocal microscope (Leica, Wetzlar, Germany) for GFP (excitation, 488 nm; emission, 518–524 nm) or for chlorophyll fluorescence (excitation, 488 nm; emission, 680–690 nm).

Isolation and Complementation of the Arabidopsis AtmenG Mutant—An *Arabidopsis* line carrying a T-DNA insertion in the At1g23360 locus (GABI_565F06) was obtained from the GABI-Kat collection in Cologne, Germany (23). PCR using gene-specific primers (PD464, 5′-AGA AAT GTG TAG CTT GGC TTG ATT-3′; PD465, 5′-GTT ACT GGT TGT AGC AAG TTT GGA-3′) with genomic DNA from wild type or a heterozygous line resulted in amplification of a 1630-bp fragment, in contrast to homozygous lines where no band was produced. A 670-bp fragment containing part of the T-DNA insertion could be amplified by PCR with the primers PD464 and PD394 (T-DNA left boarder primer; 5′-CCC ATT TGG ACG TGA ATG TAG ACA C-3′) in homozygous or heterozygous lines. For complementation, the ORF was released from pBluescript-At1g23360 with KpnI and BamHI, ligated into the corresponding sites of the binary vector pBINAR containing a CaMV ^{35}S promoter (24) and transferred into the *Arabidopsis AtmenG* mutant via *Agrobacterium*-mediated transformation (25). Transformed plants were selected on kanamycin-containing medium, and At1g23360 expressing lines identified by Northern blot analysis. Total RNA was isolated from leaves and used for Northern blot hybridization with a ^{32}P-labeled At1g23360 cDNA as a probe following standard protocols (26).

Incorporation of [1-^{3}H]Phytol into Arabidopsis Seedlings—Seedlings of *Arabidopsis* (10 days old) were incubated in 20 mM MES-KOH, pH 6.8, 0.2% Tween 80 with 100 pmol of [1-^{3}H]phytol (20 Ci/mmol, American Radiolabeled Company/BioTrend, Cologne, Germany) and lipids extracted as previously described (27). Radioactive lipids were separated by TLC (hexane/diethylether/acetic acid; 85:15:1) including standards (phytol, α-tocopherol, phylloquinone) and visualized with a

β-scanner (Automatic TLC Linear Analyzer, Berthold, Wildbad, Germany).

Quantification of Chlorophyll, Photosynthetic Pigments, Anthocyanin, and Tocopherol—Chlorophyll in leaves was measured photometrically in 80% acetone (28). Photosynthetic pigments were extracted from leaves with acetone and quantified by HPLC (29). Anthocyanin was extracted from leaves with 1-propyl alcohol/1% HCl/water (18:1:81), the extracts boiled for 3 min, and incubated in darkness for 2 h. Subsequently, anthocyanin was quantified photometrically according to the equation ($A_{535} - 2 \times A_{650}$) per g fresh weight (30). Tocopherol was measured by fluorescence HPLC (31).

Chloroplast Isolation and Fractionation—Chloroplasts were isolated from *Arabidopsis* WT and *AtmenG* leaves by homogenization (32). After hypotonic rupture of chloroplasts, subplastidial compartments were separated by centrifugation using a standard sucrose density gradient, and subfractions of 1 ml were collected (32). Immunoblot analysis (with antibodies against plastoglobulin AtPGL35, the translocator of the outer envelope AtToc75, chlorophyll a binding protein, CAB) was performed on subfractions of the sucrose gradient to assess the distribution of plastoglobules, envelopes, and thylakoids. The results of immunoblots were analogous to those published in Fig. 2 of Vidi *et al.* (32), and the gradient subfractions were pooled accordingly into five fractions (F1–F5). The upper gradient fractions F1 (subfractions 1–6 or 1–5 for WT or *AtmenG*, respectively) and F2 (subfractions 7–13 or 6–17) contained mostly plastoglobules. Envelopes and low amounts of thylakoids were found in F3 (subfractions 14–19 or 18–21). Fraction F4 (subfractions 20–23 or 22–25) contained envelopes and thylakoids, and F5 (subfractions 24–29 or 26–29) mostly thylakoids (32). Lipids were extracted from the five fractions with chloroform/methanol (2:1), and total fatty acids and phylloquinone were quantified by GC (33) and fluorescence HPLC (see above), respectively.

Differential Chlorophyll Absorption Measurement of PSI in Leaf Discs—As a measure for the content of photochemically active PSI, the transmission change at 830–870 nm, resulting from photo-oxidation of P_{700}, was determined in leaf discs of *Arabidopsis*. The transmission changes ($\Delta I/I$) were corrected for the contribution of plastocyanin, determined at 870–950 nm (34), but using an optimized new generation pulse amplified modulation (PAM) system (Dual-PAM, plastocyanin-P_{700} version, Heinz Walz, Effeltrich, Germany), which allows simultaneous determination of the difference transmission signals arising from plastocyanin and P_{700}.[4] Using pre-illuminated *Arabidopsis* leaves with fully active Calvin cycle to avoid an acceptor-side limitation of PSI oxidation, P_{700} and plastocyanin were pre-oxidized by 10-s illumination with weak far-red light selectively exciting PSI, followed by a strong saturating red light pulse (100-ms duration, 6000 μmol m^{-2} s^{-1}), resulting in complete photooxidation of P_{700} and plastocyanin and their subsequent reduction after the end of the light pulse. The maximal transmission changes between fully oxidized and fully reduced states were calculated. After transmission measurement, the

---

[4] M. A. Schöttler, C. Flügel, W. Thiele, and R. Bock, submitted manuscript.

leaf segment was punched, frozen in liquid nitrogen, and chlorophyll content determined (28). Transmission changes were normalized to a chlorophyll content of 1 mg.

Thylakoid Isolation and Quantification of PSI, PSII, and Cyt b_6/f—Thylakoid membranes were isolated as described (36). Thylakoid proteins were separated by SDS-polyacrylamide gel electrophoresis and transferred to immunoblot membranes, and blots were probed with polyclonal antiserum raised against PsaC (PS I), PsbD (PS II), or PetA (Cyt b_6/f).[4]

PSI, PSII, or Cyt b_6/f were determined in isolated thylakoids by difference absorption measurements (36). Briefly, PSI was measured from P_{700} redox changes after thylakoid membrane solubilization with 0.2% (w/v) β-dodecylmaltoside (50 μg Chl ml^{-1}). Ascorbate was used as electron donor to maintain P_{700} in a fully reduced state in the dark, and methylviologen was used as electron acceptor during photooxidation after application of a saturating red light pulse (6000 μmol m^{-2} s^{-1}, 200-ms duration).

For measurements of the cytochromes in PSII and Cyt b_6/f, thylakoid membranes were de-stacked in a low salt buffer containing 0.03% (w/v) β-dodecylmaltoside to eliminate light scattering effects. The cytochromes were oxidized with ferricyanide and subsequently reduced with ascorbate and dithionite, resulting in reduction of Cyt f and the high potential form of Cyt b_{559} (HP, ascorbate-ferricyanide difference absorption spectrum) and reduction of cytochrome b_6 and the low potential form of Cyt b_{559} (LP, dithionite-ascorbate), respectively. Absorption spectra were recorded using a Jasco J-550 spectrophotometer with head-on photomultiplier between 575 and 540 nm, and difference absorption spectra were deconvoluted using reference spectra and difference absorption coefficients for the cytochromes. PSII contents were calculated from the sum of the Cyt b_{559} HP and LP difference absorption signals (37).

Measurement of PSI Electron Transfer Rate—PSI electron transfer activity was measured in thylakoids by recording oxygen consumption in continuous white light (5000 μmol m^{-2} s^{-1}, halogen lamp) with a Clark-type electrode. Briefly, PSII activity in thylakoids was inhibited with 3-(3′,4′-dichlorophenyl)-1,1-dimethylurea (DCMU, 100 μM), and electron transfer from ascorbate (10 mM) via the mediator N,N,N',N'-tetramethylphenylenediamine dihydrochloride (TMPD, 100 μM) and plastocyanin to PSI was measured. Methylviologen (100 μM) was added as electron acceptor, resulting in the reduction of O_2 to H_2O_2. Because catalase activity was inhibited by the addition of 1 mM NaN$_3$, PSI activity could be calculated from O_2 reduction (38).

Low Temperature (77 K) Chlorophyll Fluorescence—Low temperature (77 K) chlorophyll a fluorescence emission spectra were recorded with a Jasco F6500 fluorometer with a red-sensitive photomultiplier. Isolated thylakoids were diluted to a chlorophyll concentration of 10 μg of Chl ml^{-1}, fluorescence was excited at 430 nm and emission spectra measured from 660 to 800 nm. Spectra were corrected for the instrumental response of the photomultiplier and normalized to the PSII emission signal at 685 nm.

Measurements of PS II Quantum Yield—Chlorophyll fluorescence was measured with a pulse amplitude modulation fluo-
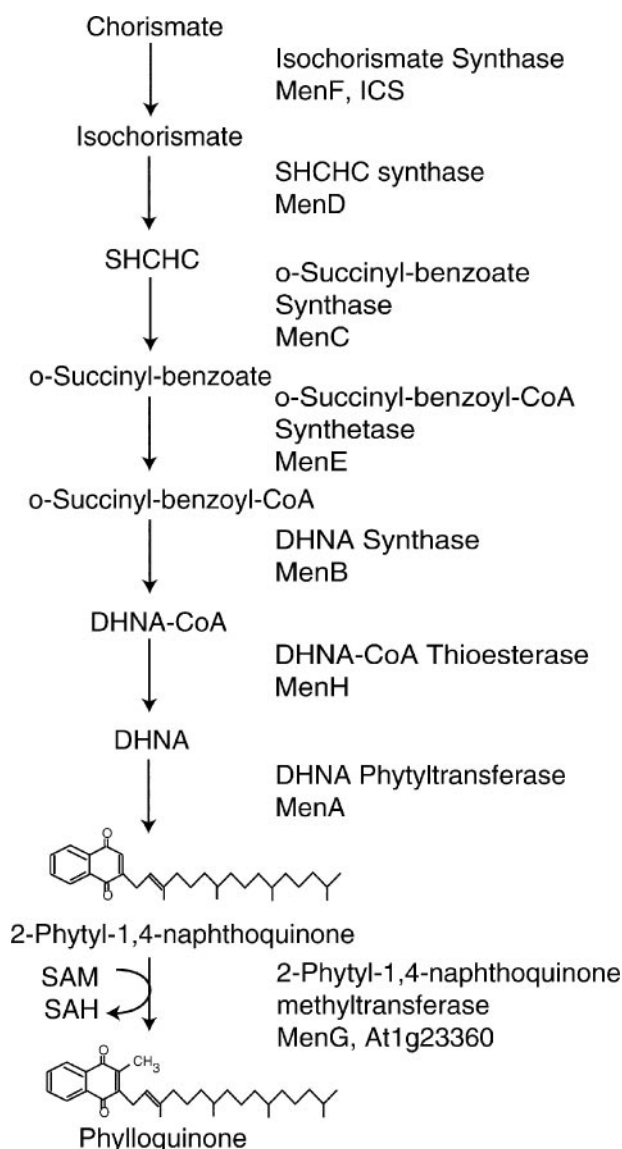

FIGURE 1. **Pathway of phylloquinone synthesis.** The reactions of phylloquinone biosynthesis are based on the pathway described for cyanobacteria and *Arabidopsis* (7, 10, 15). *SHCHC*, 2-succinyl-6-hydroxy-2,4-cyclohexadiene-1-carboxylate; *SAM*, S-adenosyl-methionine; *SAH*, S-adenosyl-homocysteine.

rimeter (Imaging PAM; Heinz Walz, Effeltrich, Germany) with dark-adapted plants. Fluorescence light response curves were recorded after a 5-min exposure of the leaves to the photosynthetically active radiation (PAR) as indicated. PSII quantum yield was calculated according to the equation $(F_{m'} - F)/F_{m'}$ (39).

RESULTS

Identification of the Gene Encoding PNQ Methyltransferase in Arabidopsis—The pathways of menaquinone and phylloquinone biosynthesis have been studied in bacteria, and most of the genes have been functionally characterized (Refs. 7, 10, and 15 and Fig. 1). The ultimate step of phylloquinone synthesis, the methylation of 2-phytyl-1,4-naphthoquinone, is encoded by the *menG* gene (sll1653) in *Synechocystis* (10). A gene survey performed for genes of isoprenoid metabolism revealed the existence of up to four *menG*-like sequences in the *Arabidopsis*
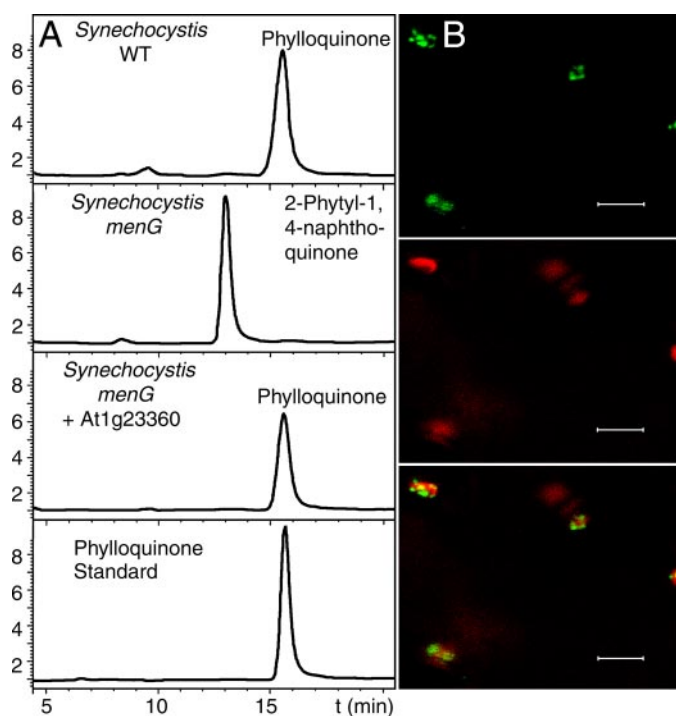
FIGURE 2. **The *Arabidopsis* protein At1g23360 harbors PNQ methyltransferase activity and localizes to the chloroplast.** *A*, the ORF At1g23360 was introduced into the *Synechocystis menG* mutant sll1653 deficient in PNQ methyltransferase. Phylloquinone was measured by fluorescence HPLC. Four chromatograms are shown for WT *Synechocystis* (*top*), *Synechocystis menG* mutant (*second*), *Synechocystis menG* mutant carrying the At1g23360 ORF (*third*), and phylloquinone standard (*bottom*). The peaks at 13 and 15.5 min were identified as PNQ and phylloquinone, respectively. *B*, a fusion of *At1g23360* with coding region of the GFP was transiently expressed in *Arabidopsis* leaves after ballistic transformation, and subcellular localization analyzed by confocal fluorescence microscopy. GFP fluorescence (*top*), chlorophyll fluorescence (*center*), merged images (*bottom*). *Scale bars*, 8 μm.

genome, At1g23360, At3g02770, At5g16450, and At5g56260 (40). Pairwise comparison demonstrated that the protein sequence of At1g23360 is by far the most similar sequence to sll1653 (47.9% amino acid sequence identity), whereas the other three *Arabidopsis* sequences showed identities with sll1653 of only 11–13%.

To study the At1g23360 gene product at the functional level, the corresponding full-length cDNA was amplified by PCR from cDNA derived from *Arabidopsis* mRNA. Complementation of a *Synechocystis* mutant deficient in the orthologous open reading frame sll1653 (10) was attempted to functionally characterize the At1g23360 gene product from *Arabidopsis*. To this end, the sll1653 gene of *Synechocystis* was first inactivated by insertional mutagenesis, and phylloquinone content determined by fluorescence HPLC. As shown in Fig. 2*A*, the *Synechocystis menG* mutant was totally devoid of phylloquinone, but a new peak was observed with earlier retention time, which was identified as PNQ (10). Heterologous expression of the *Arabidopsis* At1g23360 cDNA in the *Synechocystis* sll1653 mutant resulted in the disappearance of PNQ, and in the concomitant observation of a peak co-migrating with phylloquinone. Therefore, the At1g23360 protein must be capable of converting PNQ to phylloquinone demonstrating that it harbors PNQ methyltransferase activity.

The At1g23360 Protein Localizes to Chloroplasts—The enzymatic activity of PNQ methyltransferase was previously localized to the envelope membranes of spinach chloroplasts (11). Therefore, it was expected that the At1g23360 protein localizes to chloroplasts. As compared with the orthologous *Synechocystis* sequence sll1653, the At1g23360 protein contains an N-terminal extension of 37 amino acids. This N-terminal extension was predicted to contain a signal peptide for import into chloroplasts with a putative cleavage site C-terminal to Lys[30] according to the ChloroP1.1 program (Ref. 41). To determine the subcellular localization experimentally, the entire At1g23360 coding sequence was translationally fused to the N-terminal sequence of the GFP gene and transiently transferred into *Arabidopsis* leaf mesophyll cells (Fig. 2*B*). Examination by confocal microscopy revealed that the green fluorescence of the At1g23360-GFP fusion protein co-localized with chlorophyll fluorescence, indicating that the At1g23360 protein localizes to chloroplasts (Fig. 2*B*).

Isolation and Complementation of an Arabidopsis AtmenG Mutant—To study the functional significance of the last step of phylloquinone synthesis in higher plants, an *Arabidopsis* mutant carrying a T-DNA insertion in the gene At1g23360 was obtained. A homozygous line was isolated by PCR screening using primer combinations for the genomic At1g23360 locus or for a T-DNA fragment containing flanking genomic sequences (Fig. 3*A*). Sequence analysis confirmed that the mutant harbors a T-DNA insertion in the 7th exon of the At1g23360 gene. The At1g23360 mRNA was not detectable in homozygous *AtmenG* mutant plants, in contrast to WT, where a weak band at around 800 bases was observed (Fig. 3*B*). To test whether the *AtmenG* mutant can be phenotypically complemented by expression of the candidate *Arabidopsis menG* gene product, the mutant was transformed with the At1g23360 ORF under the control of the CaMV ^{35}S promoter, and transgenic plants with high levels of At1g23360 mRNA were identified by Northern blot analysis (Fig. 3*B*).

Fluorescence HPLC measurements revealed that *AtmenG* mutant leaves were totally devoid of phylloquinone (Fig. 3*C*). A new peak with shorter retention time was detected, which was tentatively identified as PNQ. The amount of PNQ in *AtmenG* was even higher than that of phylloquinone in WT leaves (5.71 $\pm$ 0.39 and 4.56 $\pm$ 0.48 nmol g^{-1} FW, respectively; Fig. 3*C*). Furthermore, fluorescence HPLC analysis showed that all PNQ was converted into phylloquinone by overexpression of the At1g23360 cDNA in the *AtmenG* mutant background.

During phylloquinone synthesis, the phytyl group of phytyldiphosphate is transferred onto DHNA by DHNA phytyltransferase (Refs. 11 and 15 and Fig. 1). Free phytol can serve for the production of phytyl containing lipids (tocopherol, fatty acid phytyl esters) in *Arabidopsis* after phosphorylation to phytyldiphosphate (27, 42). To test whether free phytol can be employed for phylloquinone synthesis and to identify different phytol-containing reaction products, seedlings of *Arabidopsis* WT, *AtmenG*, and *AtmenG*-At1g23360 were incubated with radioactive [1-^{3}H]phytol, followed by lipid separation by TLC. In wild type and complemented plants, a radioactive band was observed that co-migrated with a phylloquinone standard (Fig. 3*D*). This band was absent in the *AtmenG* mutant, but another
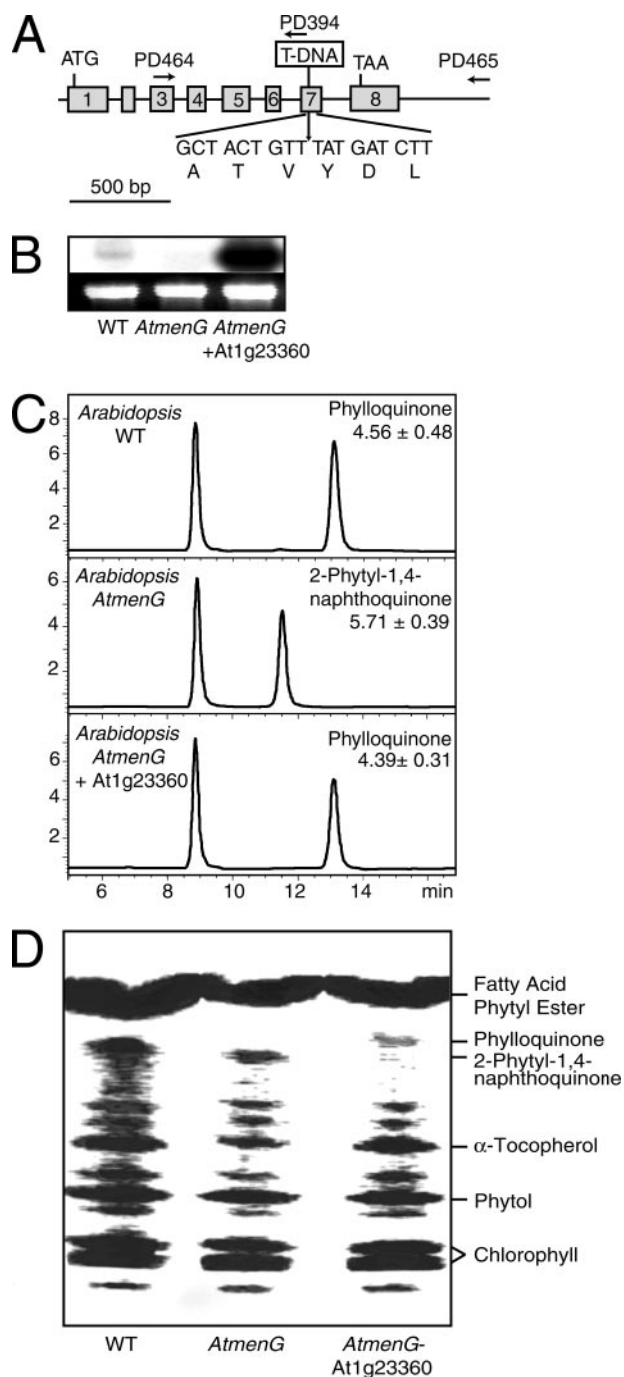
FIGURE 3. **Isolation of the *Arabidopsis AtmenG* mutant.** *A*, intron/exon structure of the gene *At1g23360*. The location of the T-DNA insertion in the 7th exon in mutant line *AtmenG* (GABI_565F06) was confirmed by PCR with the primers PD464 and PD394 and sequencing. *B*, detection of the *At1g23360* mRNA in WT, *AtmenG*, and in the *AtmenG* line complemented with the At1g23360 ORF. The *top panel* shows the Northern blot after hybridization to the At1g23360 cDNA, the *lower panel* shows the 26 S rRNA bands in the agarose gel prior to blotting. *C*, phylloquinone content in WT (*top*), *AtmenG* mutant (*center*), and in *AtmenG* complemented with the At1g23360 ORF (*bottom*) was measured by fluorescence HPLC using menaquinone-4 (9 min) as internal standard. Numbers indicate quinone content in μg g^{-1} fresh weight (mean ± S.D.; $n = 3$). *D*, phylloquinone synthesis is affected in *AtmenG*. Seedlings of WT, *AtmenG*, and complemented plants (*AtmenG*-At1g23360) were incubated with [1-³H]phytol, lipids separated by TLC, and visualized by autoradiography. Radioactive phytol was incorporated into fatty acid phytyl esters, phylloquinone, tocopherol, and chlorophyll *a* and *b*. In the *AtmenG* mutant, radioactive phytol was not incorporated into phylloquinone, but into a compound with a lower Rf value, presumably 2-phytyl-1,4-naphthoquinone.

band with a slightly lower Rf accumulated, which was tentatively identified as PNQ. In conclusion, the *AtmenG* mutant carries a full knock-out mutation of the PNQ methyltransferase gene resulting in the loss of phylloquinone synthesis with a concomitant accumulation of the precursor PNQ.

Subplastidial Distribution of Phylloquinone and PNQ—To estimate the amounts of phylloquinone in subplastidial compartments, chloroplasts were isolated from *Arabidopsis* WT leaves, and after rupture in hypotonic buffer, subplastidial fractions separated via sucrose gradient centrifugation. Immunoblot analysis with antibodies to marker proteins revealed that the distribution of plastidial compartments in the gradient subfractions was analogous to that observed previously (32). Five fractions were pooled containing plastoglobules, envelopes, and thylakoid membranes. Subsequently, total fatty acids and phylloquinone were measured in these five fractions, and the ratio of phylloquinone to fatty acids and the relative distribution of phylloquinone calculated. Fig. 4*A* shows that a large amount of phylloquinone (about 60%) localizes to the thylakoids (F4, F5), but a substantial quantity (30%) was also associated with the plastoglobules (F1, F2). The ratio of phylloquinone to fatty acids was highest in the plastoglobule fraction F1 (0.004) and much lower in the thylakoid fraction F5 (0.002; Fig. 4*C*). The low phylloquinone to fatty acid ratio in thylakoids can be explained by the high proportion of galactolipids.

Furthermore, the distribution of PNQ was measured in chloroplast fractions derived from *AtmenG* plants. The amount of PNQ in thylakoids (F4, F5) was about 25%, and in plastoglobules (F1, F2) ca. 70% (Fig. 4*B*). The ratio of PNQ to total fatty acids was ca. 0.016 in the plastoglobules fraction F1, and much lower in the other gradient fractions. Therefore, the relative distribution of PNQ in *AtmenG* differs from that of phylloquinone in WT, because PNQ is highly enriched in plastoglobules compared with thylakoids.

The AtmenG Mutation Affects Growth and Anthocyanin Accumulation—*AtmenG* plants showed significantly reduced growth when raised under normal light of 150 μmol m^{-2} s^{-1} (Fig. 5*A*). Growth reduction of *AtmenG* was restored after transformation with the At1g23360 cDNA indicating that it was caused by a block in PNQ methyltransferase activity. High light conditions are known to affect the efficiency of photosynthesis, resulting in photoinhibition of PSII and stimulation of different photoprotective mechanisms. For example, anthocyanin, a flavonoid pigment localized to the vacuoles of mesophyll cells, accumulates at high light (43, 44). Plants were transferred to high light (550 μmol m^{-2} s^{-1}) for 4 days to study the effect of the replacement of phylloquinone with PNQ on photosynthesis and overall plant physiology. WT *Arabidopsis* plants showed a red leaf color at high light (Fig. 5*A*). This color originated from anthocyanin accumulation as demonstrated by photometric measurements (Fig. 5*B*). By contrast, the accumulation of anthocyanin was compromised in *AtmenG* plants. Chalcone synthase represents one of the key enzymes in anthocyanin synthesis, and the *CHS1* gene is known to be strongly expressed during high light exposition (43). Northern analysis confirmed that *CHS1* expression in WT increased under high light, but it was reduced in *AtmenG* compared with WT and the complemented line. Therefore, phylloquinone deficiency affects the
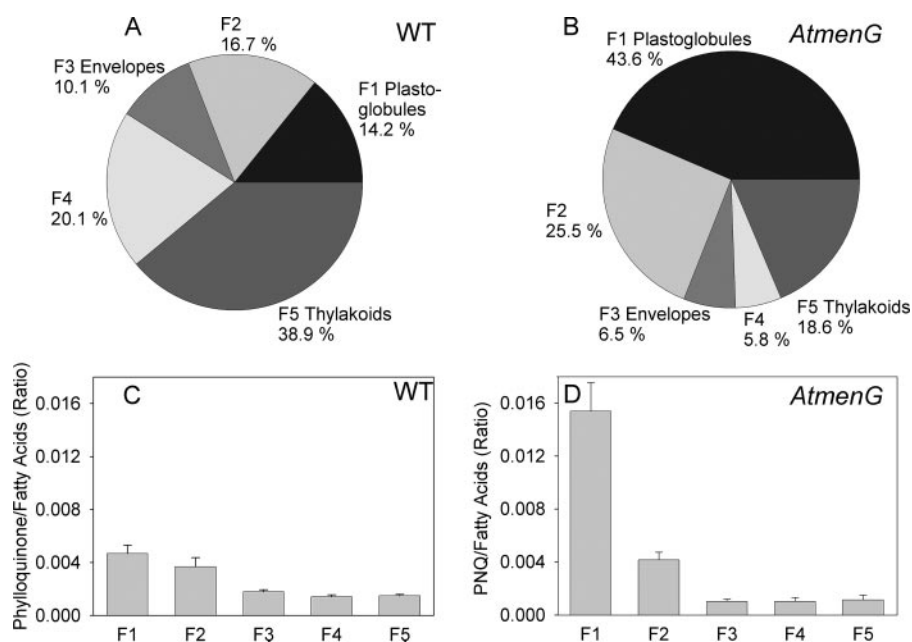
FIGURE 4. **Distribution of phylloquinone and PNQ to different chloroplast fractions from WT and AtmenG.** Chloroplasts were isolated from WT and *AtmenG* plants and after rupture, subplastidial fractions (*F1–F5*) isolated by gradient centrifugation. The distribution of subplastidial membranes was analyzed by immunoblot using antibodies against PGL-35 (plastoglobules), envelope (AtToc75), and thylakoids (CAB). Fractions F1 and F2 contained mostly plastoglobules, F3 envelopes, F4 with some envelopes and thylakoids, and F5 with mostly thylakoids (32). Phytylnaphthoquinones were measured by fluorescence HPLC, and total fatty acids by GC of methyl esters. *A*, distribution of phylloquinone to chloroplast fractions in WT; *B*, distribution of PNQ to chloroplast fractions in *AtmenG*; *C*, ratio of phylloquinone to fatty acids in WT; *D*, ratio of PNQ to fatty acids in *AtmenG*. Data represent mean of three measurements and S.D.
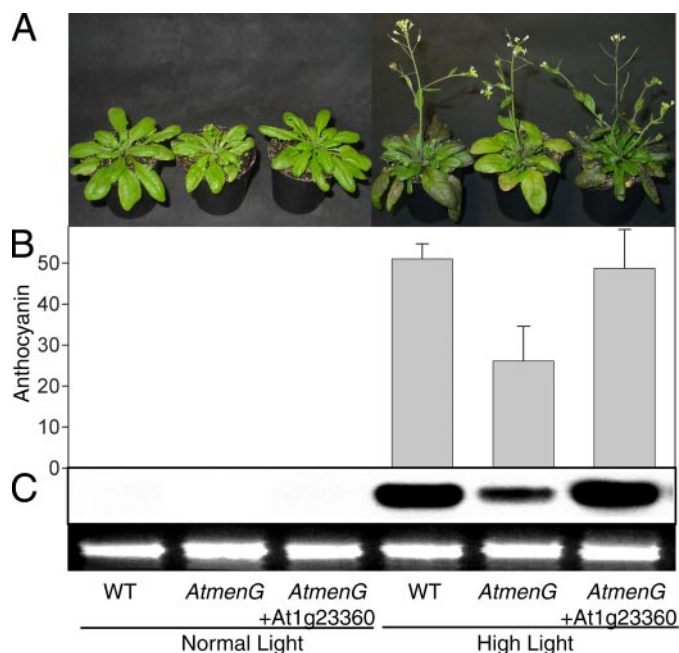

FIGURE 5. **Anthocyanin accumulation under high light is attenuated in AtmenG.** *A*, phenotypic comparison of *Arabidopsis* WT, homozygous *AtmenG*, and *AtmenG* plants complemented with At1g23360. Plants were grown under normal light (150 μmol m^{-2} s^{-1}) for 4 weeks (*left*) or raised at normal light for 24 days and then exposed to high light (550 μmol m^{-2} s^{-1}) for an additional 4 days. *B*, anthocyanin content in leaves calculated as (A_{535} − 2 × A_{650}) g^{-1} FW. Values show means and S.D. from at least three measurements. *C*, expression of chalcone synthase (*CHS1*) in leaves. The *top panel* shows the Northern blot signal after hybridization to the *CHS1* EST T20563 (At5g13930), the *lower panel* shows a photo of the rRNA band in the agarose gel.

light-dependent stimulation of anthocyanin synthesis in *AtmenG*, presumably by interfering with transcriptional activation of key pathway genes (*CHS1*).

Photosystem I Abundance Is Decreased in AtmenG—Phylloquinone is an integral constituent of PSI where it serves as electron carrier in the P$_{700}$ reaction center. Thus, it was expected that replacement of phylloquinone with its unmethylated form might affect PSI stability and abundance. To analyze the composition of photosynthetic units in thylakoid membranes, the amounts of chlorophylls and carotenoids were quantified (Table 1). In plants raised under normal light (150 μmol m^{-2} s^{-1}), the contents of chlorophyll and carotenoids were very similar in WT and *AtmenG*. To assess the abundance of PSI (PsaC), PSII (PsbD), and Cyt b_6/f (PetA) complexes, immunoblot analysis was done for subunits known to be essential for the assembly of the individual complexes in photosynthetic eukaryotes (Fig. 6*A*). The band intensity for these three proteins was very similar in WT, *AtmenG*, and in complemented mutant plants raised under normal light. Low temperature (77 K) chlorophyll fluorescence of thylakoids can be employed to estimate the relative chlorophyll distribution between PSI and PSII. When 77 K fluorescence was normalized to 1 at 685 nm, a characteristic wavelength for PSII fluorescence, differences in PSI abundance relative to PSII can be observed at the peak of 730 nm, which is indicative for PSI. As shown in Fig. 6*B* (*upper panel*) the amount of PSI was very similar for WT, *AtmenG*, and complemented plants raised at normal light.

After high light exposure for 4 days, the amount of chlorophyll in *AtmenG* decreased to 963 μg g^{-1} FW as compared with 1172 and 1162 in wild type and complemented plants, respectively (Table 1). Western analysis revealed that the amount of PsaC protein was reduced in *AtmenG* plants exposed to high light, but the amounts of PsbD and PetA remained similar to wild type and complemented plants. Furthermore, the PSI maximum at 730 nm in 77K fluorescence was reduced in *AtmenG* plants raised at high light (Fig. 6*B*, *lower panel*). Taken together, the reduction in chlorophyll content observed in *AtmenG* under high light can predominantly be attributed to a decrease in PSI abundance, while the other components of the photosynthetic apparatus (PSII, Cyt b_6/f) remain similar to wild type.

The content of active PSI reaction centers (P$_{700}$ content) was measured by difference absorption spectroscopy in leaf discs of *Arabidopsis*. As shown in Fig. 7*A*, the difference absorption signal for P$_{700}$ per chlorophyll was slightly reduced in *AtmenG*

TABLE 1

Photosynthetic pigments and lipid antioxidants in the *AtmenG* mutant

Plants (WT, *AtmenG*, complemented mutant plants) were raised at normal or high light as indicated in the legend to Fig. 5. Chlorophyll $a+b$ (Chl $a+b$, in g^{-1} FW), the chlorophyll a-to-b ratio (Chl a/b) in leaves was measured photometrically. The carotenoid contents were determined by HPLC and are presented in mmol mol^{-1} Chl. Values show means and S.D. from at least three measurements.

	Normal light			High light		
	WT	*AtmenG*	*AtmenG*-At1g23360	WT	*AtmenG*	*AtmenG*-At1g23360
Chl $a+b$	1338 ± 121	1342 ± 136	1334 ± 175	1172 ± 125	963 ± 103	1162 ± 125
Chl a/b	3.1 ± 0.1	3.1 ± 0.1	3.0 ± 0.1	2.4 ± 0.3	2.7 ± 0.5	2.6 ± 0.2
Neoxanthin	31.2 ± 1.4	31.8 ± 4.4	31.1 ± 5.3	34.6 ± 5.6	32.3 ± 1.8	32.9 ± 2.7
Lutein	105.5 ± 5.4	108.8 ± 15.3	107.3 ± 15.8	121.9 ± 18.2	119.4 ± 5.7	110.3 ± 10.9
β-Carotene	69.2 ± 3.4	65.0 ± 5.2	69.6 ± 10.2	77.8 ± 11.0	74.1 ± 2.6	79.9 ± 7.1
V+A+Z[a]	34.4 ± 1.9	41.5 ± 9.3	39.8 ± 7.1	55.7 ± 11.5	73.4 ± 4.4	54.7 ± 5.6
(A+Z)/(V+A+Z)[b]	0.186 ± 0.013	0.186 ± 0.030	0.165 ± 0.004	0.224 ± 0.084	0.451 ± 0.102	0.153 ± 0.030
Tocopherol[c]	8.0 ± 2.0	6.0 ± 1.0	8.2 ± 2.5	27.4 ± 7.3	19.8 ± 3.6	22.6 ± 2.9

[a] V+A+Z, sum of xanthophyll-cycle pigments (V, violaxanthin; A, antheraxanthin; Z, zeaxanthin; mmol mol^{-1} Chl).

[b] (A+Z)/(V+A+Z), de-epoxidation status of xanthophyll-cycle pigments (ratio).

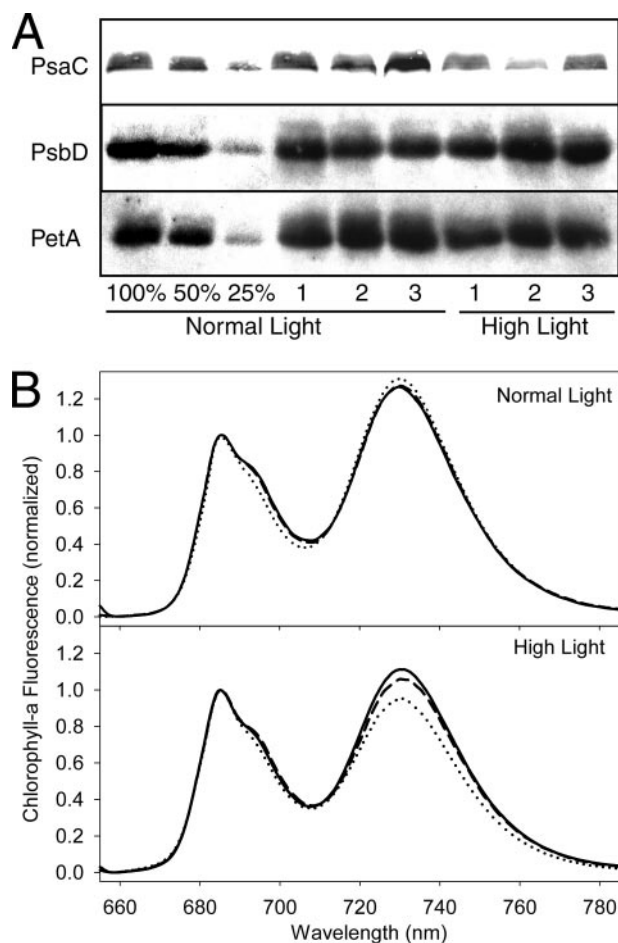[c] Tocopherol was measured by fluorescence HPLC (μg g^{-1} FW).

FIGURE 6. **Photosystem I abundance is affected in *AtmenG* plants under high light.** *A*, immunoblots of thylakoid proteins probed with antibodies against PsaC (PS I), PsbD (PS II), or PetA (Cyt b_6/f). The *first three lanes* contain 100, 50, and 25% of wild-type thylakoid protein. *Lane 1*, WT; *lane 2*, *AtmenG* mutant; *lane 3*, *AtmenG* complemented with At1g23360. *B*, low temperature (77 K) fluorescence spectra of thylakoids derived from plants raised at normal or high light. Chlorophyll fluorescence at 685 nm (PS II band) was normalized to 1. WT (*continuous line*); *AtmenG* (*dotted line*), *AtmenG*-At1g23360 (*dashed line*). Plants were raised at normal or high light as described in the legend to Fig. 5.

as compared with WT and complemented plants (*AtmenG*-At1g23360), and this effect became more severe when plants were exposed to high light. The contents of the different photosynthetic complexes, PSI, PSII, and Cyt b_6/f were quantified

in thylakoids by differential absorption spectroscopy. In accordance with data obtained for leaf discs (Fig. 7*A*), the amount of PSI per chlorophyll was slightly decreased in thylakoids exposed to normal light (Fig. 7*B*), and it was strongly reduced at high light. On the other hand, the PSII and Cyt b_6/f contents were very similar at normal light, and slightly increased at high light in *AtmenG* (Fig. 7, *C* and *D*), a consequence of the reduced chlorophyll distribution to PSI.

To obtain a measure for the activity of electron flow through PSI, thylakoids were purified from chloroplasts and used for electron transfer assays with ascorbate/TMPD and methylviologen as electron donor and acceptor, respectively, while PSII activity was inhibited with DCMU. Oxygen consumption was measured with a Clark-type electrode. This assay is strongly dependent on plastocyanin availability per PSI, as the P$_{700}$ reduction by plastocyanin is the rate-limiting step of the ascorbate/TMPD assay. Whereas the plastocyanin-PSI ratios were identical in all low light grown lines (not shown), in high light, the ratio of plastocyanin to PSI was strongly increased in *AtmenG*, because of the reduced PSI content (data not shown). Therefore, the assays were only conducted with thylakoids from plants grown at normal light. As shown in Fig. 7*E*, PSI electron transfer rates (on a chlorophyll basis) were slightly decreased in *AtmenG* plants raised at normal light. Considering the slight reduction in PSI content per chlorophyll (Fig. 7, *A* and *B*), electron transfer rates per PSI of WT and *AtmenG* were indistinguishable. In conclusion, differential absorption measurements of leaf discs and thylakoids, and PSI electron transport activity determinations revealed a slight reduction in PSI abundance in *AtmenG* plants at normal light, and this decrease became even more severe when plants were exposed to high light. However, the electron transport capacity per PSI unit was not affected by replacement of phylloquinone in *AtmenG*. The amounts of the other photosynthetic complexes were not decreased.

Exposure to High Light Affects PSII Quantum Yield and Xanthophyll Cycle Pigment Composition in AtmenG—To obtain a measure for the efficiency of light conversion into chemical energy, chlorophyll fluorescence was measured with plants exposed to different light intensities and the photosynthetic quantum yield of PSII was calculated. No difference in quantum yield was detected for dark adapted plants (Fig. 8), indicating that PSII efficiency was not altered in *AtmenG*. The quantum
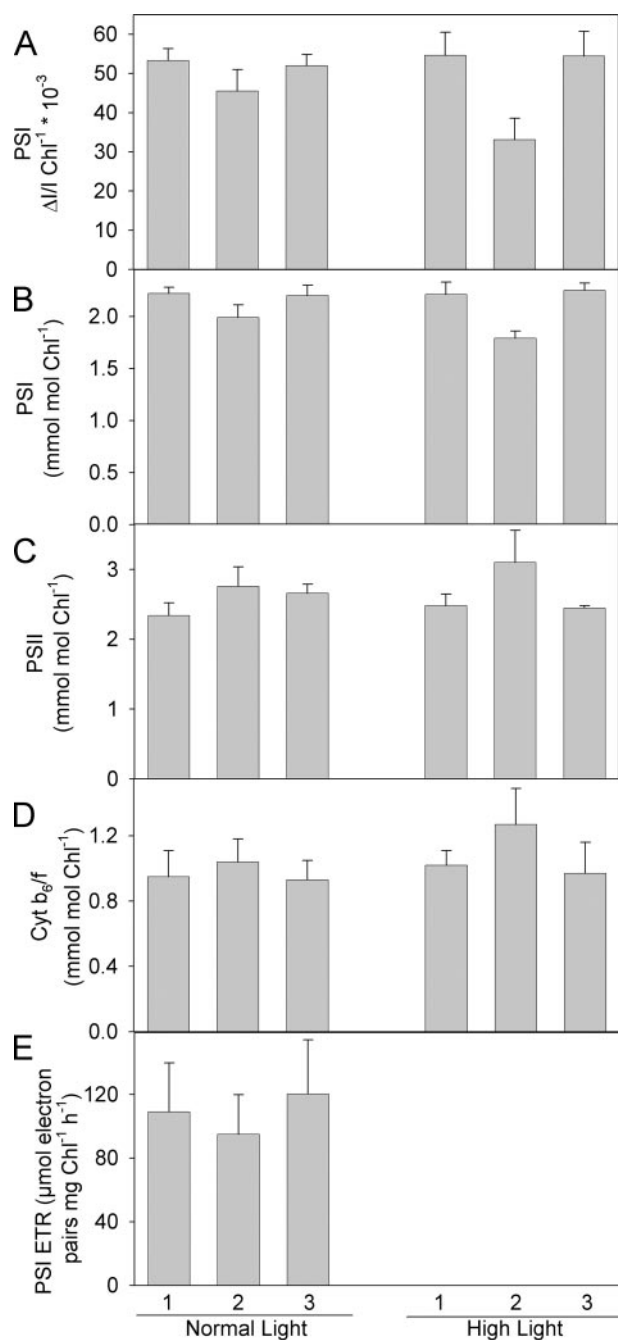
FIGURE 7. **Photosystem I abundance and activity in *AtmenG* plants.** *A*, PSI content in leaf discs was measured by difference absorption spectroscopy of P700 chlorophyll. Light-induced changes in P_{700} transmission signals ($\Delta I/I$) are calculated based on total chlorophyll content. The abundance of photosynthetic complexes PS I (*B*), PSII (*C*), and Cyt b_6/f (*D*) was determined by difference absorption spectroscopy of thylakoid membranes. *E*, electron transfer activity of PSI in thylakoids was measured with ascorbate and methylviologen as electron donor and acceptor, respectively. Oxygen evolution was recorded with a Clark electrode. WT, *AtmenG*, and complemented *AtmenG* plants were grown under normal or high light as described in the legend to Fig. 5.
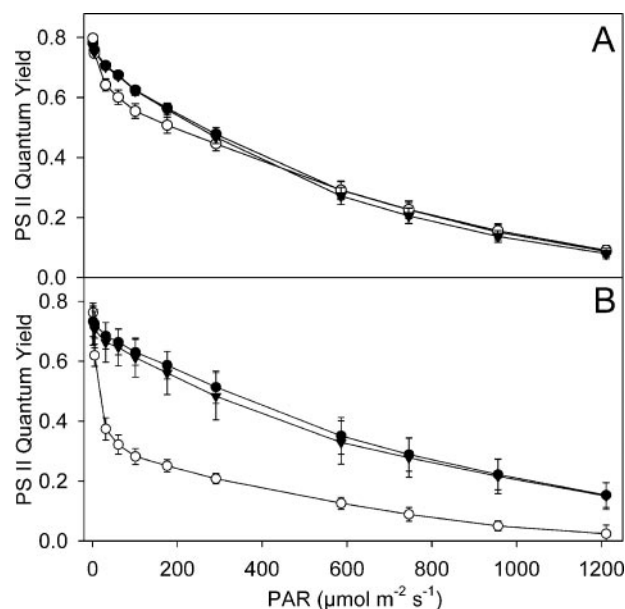

FIGURE 8. **Light response curves for WT, *AtmenG* mutant, and complemented *AtmenG* plants.** Dark-adapted plants were exposed to different light conditions for 5 min and employed for chlorophyll fluorescence measurements. Effective PSII quantum yield, ($F_{m'} - F$)/$F_{m'}$ is represented as means $\pm$ S.E. of five measurements. ●, WT; ○, *AtmenG*; ▼, *AtmenG*-At1g23360 (complemented mutant). *PAR*, photosynthetically active radiation. *A*, plants grown under normal light. *B*, plants exposed to high light (see legend to Fig. 5).

To address the question whether changes in photosynthetic characteristics of the thylakoid membrane in *AtmenG* affect the antioxidant status of the plant, tocopherol was measured in leaves of plants exposed to normal or high light (Table 1). The amount of tocopherol in *AtmenG* plants raised at normal light was not different from WT. High light resulted in a strong increase in tocopherol in all three lines, but tocopherol content in *AtmenG* was not different from WT. These data suggest that the *AtmenG* mutation does not result in overall oxidative stress.

High light exposure resulted in an apparent increase in the pool size of xanthophyll cycle pigments violaxanthin, antheraxanthin, and zeaxanthin in *AtmenG* when calculated on a chlorophyll basis (Table 1). This apparent increase can be explained by the decrease in PSI and total chlorophyll content in *AtmenG* plants exposed to high light (Table 1). The de-epoxidation status of xanthophyll cycle pigments $(A+Z)/(V+A+Z)$ was clearly increased at high light, from 0.224 in WT to 0.451 in *AtmenG*. In conclusion, phylloquinone deficiency in *AtmenG* affected PSI abundance and PSII efficiency at high light. As a consequence, the xanthophyll cycle de-epoxidation status was increased, indicating the stimulation of photoprotective mechanisms in *AtmenG*.

DISCUSSION

The initial goal of this study was the identification of the gene encoding PNQ methyltransferase from *Arabidopsis*. Several lines of evidence support the conclusion that the gene At1g23360 encodes a genuine PNQ methyltransferase: (i) The At1g23360 cDNA is capable of complementing a *Synechocystis menG* (sll1653) loss-of-function mutant. (ii) An *Arabidopsis*

yield measured at light intensities of $50\text{–}200$ μmol m^{-2} s^{-1} was slightly reduced in *AtmenG* as compared with wild type and complemented lines (Fig. 8*A*). *AtmenG* plants raised at high light showed a severe decrease in PSII quantum yield already at low light intensities, indicating a strong restriction of linear electron flux because of the reduced PSI content (Fig. 8*B*).

Phylloquinone Methylation in Arabidopsis

AtmenG mutant carrying a T-DNA insertion in the gene At1g23360 displays phylloquinone deficiency and contains increased amounts of PNQ. (iii) Transformation of the *AtmenG* mutant with the At1g23360 ORF results in the conversion of PNQ to phylloquinone. (iv) Radioactive phytol was incorporated into phylloquinone in WT and complemented *AtmenG* plants, but into PNQ in *AtmenG* (Fig. 3*D*). Complete absence of phylloquinone from *AtmenG* suggests that *Arabidopsis* has only one functional *menG* gene and that the other three ORFs identified as weakly homologous to *menG* (38) are unlikely to specify functional PNQ methyltransferases. Our finding that even massive overexpression of *AtmenG* in the complemented mutant plants (Fig. 3*B*) does not result in phylloquinone accumulation beyond wild-type levels (Fig. 3*C*) indicates that PNQ methylation does not constitute a rate-limiting step in phylloquinone synthesis.

Two molecules of phylloquinone localize to each PSI monomer in the thylakoid membranes (1–3). Mutations in the isochorismate synthase genes of *Arabidopsis* (*ics1*, *ics2*) result in partial phylloquinone depletion, but PSI activity was affected to a lesser extent (16). It was concluded that a fraction of phylloquinone is not associated with PSI reaction centers (16). Calculations based on our results (Table 1, Figs. 3*C* and 7*C*) indicate that the ratio (mmol per mmol) of phylloquinone to PSI is about 3.1 in WT, whereas the PNQ to PSI ratio is ca. 4.4 in *AtmenG*. These two ratios exceed the theoretical value of 2.0. The excess amounts of phytylnaphthoquinones might be localized to other compartments of the chloroplast, *i.e.* the thylakoid lipid matrix, envelope membranes or to plastoglobules. Indeed, the proportion of phylloquinone in thylakoids and plastoglobules of WT was ca. 60 and 30% of total phylloquinone (Fig. 4), respectively, confirming previous data on the identification of phylloquinone in plastoglobules (45). Therefore, the excess amount of phylloquinone not associated with PSI localizes to the plastoglobules of chloroplasts. In this respect it seems unlikely that significant amounts of phylloquinone not associated with the thylakoids exist outside of plastids (*e.g.* plasma membrane) as previously suggested (16). Furthermore, the increase in PNQ in *AtmenG* as compared with phylloquinone in WT (Fig. 3*C*) can be explained by a preferred accumulation in plastoglobules (Fig. 4*D*). These results indicate that plastoglobules serve as a sink for the deposition of excess amounts of phylloquinone and its biosynthetic precursor. Furthermore, lipid trafficking must be involved in the transport of prenyl quinones from their site of synthesis, the envelope membranes, to thylakoids and plastoglobules.

The block in PNQ methyltransferase activity in *AtmenG* affects anthocyanin accumulation during high light exposure, and this effect is mediated by interfering with expression of anthocyanin synthesis genes (*CHS1*). Interestingly, a similar effect, *i.e.* the reduced accumulation of anthocyanin during high light exposure, was previously observed for other *Arabidopsis* mutants, *e.g. vte1* and *vtc2*, affected in tocopherol and ascorbate synthesis, respectively (46–48). The impact of a mutation in chloroplast lipid synthesis (*AtmenG, vte1*) on anthocyanin production is unusual given the fact that anthocyanin is synthesized in the cytosol and localizes to a different compartment, the vacuoles. Nevertheless, the accumulation of

anthocyanin is believed to be crucial in protecting the photosynthetic membrane against excess light (44). However, alterations in photosynthesis and antioxidant content do not necessarily result in anthocyanin increase (47). We presume that the altered anthocyanin accumulation in *AtmenG* originates from changes in chloroplast-to-nucleus signaling in response to high light, potentially as a consequence of the metabolic status of the cell. The photosynthetic capacity of the *AtmenG* mutant is clearly reduced at high light, and therefore, carbon assimilation presumably is also affected (Fig. 8). As chalcone synthase expression is well known to be sucrose-dependent (49), the high light-stimulated synthesis of anthocyanins in wild type and complemented plants might be explained by their higher photosynthetic efficiency, as this should result in more pronounced photoassimilate accumulation than in the *AtmenG* line.

Total absence of phylloquinone results in a drastic reduction in growth and photosynthetic efficiency in the *AtmenA* mutant of *Arabidopsis*, which is deficient in DHNA phytyltransferase (15). However, in the *AtmenG* mutant, which is also phylloquinone-deficient, growth, total chlorophyll and PSI contents, and photosynthetic efficiency were only moderately affected. This suggests that PNQ can partially replace phylloquinone as electron carrier in PSI of *AtmenG*. Similarly, in the phylloquinone-deficient *Synechocystis menG* mutant, PNQ was detected in PSI complexes where it functionally replaced phylloquinone (10). The replacement of phylloquinone with its unmethylated precursor in the PSI reaction center affects electron flow from P_{700} to the iron-sulfur cluster F_X in the *Synechocystis menG* mutant (10). The lifetime for electron transfer from Q^- to F_X is slowed from 290 ns (WT) to 600 ns (*AtmenG*), and the redox potential of PNQ is slightly more oxidizing (about 50–60 mV) than that of phylloquinone (10).

Photosynthesis in *AtmenG* was only slightly affected in plants raised at normal light (Figs. 6–8 and Table 1). This is not surprising, because in wild type the rate-limiting step of electron flux through PSI is plastocyanin binding to PSI and electron transfer to P_{700}^+ (50, 51). Therefore, only very drastic changes at the PSI acceptor side could have a significant impact on electron transfer rates through PSI. This is definitely not the case in the *AtmenG* mutant, as electron transfer from ascorbate via TMPD and plastocyanin to methylviologen/O_2 was unaltered. However, it is possible that very minor changes in the properties of the PSI acceptor side, such as those reported by Sakuragi *et al.* (10) could slightly affect the rate of side reactions, *e.g.* electron transfer to O_2 instead of ferredoxin reduction. This might lead to local oxidative damage at PSI, which is known to result in loss of the stromal PSI subunits PsaC, PsaD and PsaE from the complex, and subsequent disassembly and degradation of the entire PSI complex (35). In this context, the more pronounced decrease of PSI units in *AtmenG* under high light (Figs. 6 and 7) might be caused by accelerated PSI degradation because of oxidative damage, which cannot be compensated by *de novo* synthesis in mature *Arabidopsis* leaves (35). An alternative explanation for the reduced PSI content is decreased *de novo* synthesis, which could be caused by down-regulation of expression of nuclear PSI genes by an unknown, phylloquinone-dependent mecha-

nism. However, this scenario seems to be unlikely, as it would not explain the differential phenotype of *AtmenG* under high *versus* normal light conditions. Therefore, local oxidative damage at the PSI reaction center, because of slight alterations in the function of the PSI acceptor side, is a more likely explanation for the observed alterations in *AtmenG* photosynthesis. This scenario is also supported by the observation that PSI abundance is selectively reduced in *AtmenG*, whereas the other photosynthetic complexes accumulate to normal or slightly increased amounts, relative to wild type.

Further evidence for the scenario that oxidative stress is involved in PSI decrease can be obtained from the apparent discrepancy of PSI quantification. While PsaC immunoblot analysis (PsaC signal reduced to less than 50% of wild type at high light; Fig. 6*A*) and *in vivo* difference transmission signals originating from P_{700} (Fig. 7*A*) on the one hand indicate a strong decrease in PSI, the 77 K chlorophyll *a* fluorescence emission (Fig. 6*B*) and *in vitro* P_{700} quantification on the other hand suggest a far less pronounced decrease of PSI (Fig. 7*B*). This apparent discrepancy can be explained by close interactions of the FeS clusters F_A and F_B bound to PsaC with phylloquinone during electron transfer. Changes in phylloquinone structure in *AtmenG* that presumably cause local oxidative stress might result in damage to PsaC, as observed in the diminished immunoblot signal. Furthermore, PsaC damage can strong affect *in vivo* P_{700} difference transmission, as it is known that PsaC is required for PSI charge separation. PSI abundance as estimated from *in vitro* difference absorption spectroscopy of thylakoids is affected to a lesser extend. In this experiment, electrons from the first FeS cluster F_X bound to the reaction center dimer PsaA and PsaB of PSI can be directly transferred onto methylviologen, *i.e.* by circumventing the FeS clusters of PsaC. Furthermore, 77 K fluorescence spectroscopy reflects changes in the antenna size of PSI because low temperature fluorescence emission originates from the Lhca antenna proteins. Therefore, our data indicate that the amount of PsaC is strongly decreased in *AtmenG* plants under high light, whereas the PSI reaction center core and the PSI antenna size seem to be affected to a lesser extent.

The decrease in chlorophyll amount observed during high light can mostly be attributed to a lower content of PSI units. PSII quantum yield of *AtmenG* was similar to wild type in dark-adapted plants (Fig. 8, *A* and *B*), but was already decreased at low light intensities, indicating that the plastoquinone pool of *AtmenG* becomes overreduced during light exposure. The lack of functional PSI complexes might be the cause for the decreased electron flow through PSII. The observed change in de-epoxidation status of xanthophyll-cycle pigments indicates an increase in photoprotective mechanisms.

In conclusion, our results clearly demonstrate that methylation of phylloquinone is important for maximal photosynthetic efficiency and optimal growth when plants are raised under normal light conditions. At high light, the replacement of phylloquinone with PNQ becomes even more significant causing a decrease in PSI complexes. This in turn leads to lowered PSII efficiency and thus negatively affects the performance of the entire photosynthetic electron transfer chain.

REFERENCES

1. Jordan, P., Fromme, P., Witt, H. T., Klukas, O., Saenger, W., and Krauss, N. (2001) *Nature* **411,** 909–917
2. Ben-Shem, A., Frolow, F., and Nelson, N. (2003) *Nature* **426,** 630–635
3. Fyfe, P. K., Hughes, A. V., Heathcote, P., and Jones, M. R. (2005) *Trends Plant Sci.* **10,** 275–282
4. Guergova-Kuras, M., Boudreaux, B., Joliot, A., Joliot, P., and Redding, K. (2001) *Proc. Natl. Acad. Sci. U. S. A.* **98,** 4437–4442
5. Fromme, P., Jordan, P., and Krauss, N. (2001) *Biochim. Biophys. Acta* **1507,** 5–31
6. Food and Nutrition Board, Institute of Medicine (2003) *Dietary Reference Intakes for Vitamin C, Vitamin E, Selenium, and Carotenoids*, pp. 162–196, Natl. Acad. Press, Washington, D.C.
7. Johnson, T. W., Shen, G., Zybailov, B., Kolling, D., Reategui, R., Beauparlant, S., Vassiliev, I. R., Bryant, D. A., Jones, A. D., Golbeck, J. H., and Chitnis, P. R. (2000) *J. Biol. Chem.* **275,** 8523–8530
8. Meganathan, R. (2001) *Vitamins and Hormones* **61,** 173–218
9. Johnson, T. W., Naithani, S., Steart, C., Jr., Zybailov, B., Jones, A. D., Goldbeck, J. H., and Chitnis, P. R. (2003) *Biochim. Biophys. Acta* **1557,** 67–76
10. Sakuragi, Y., Zybailov, B., Shen, G., Jones, A. D., Chitnis, P. R., van der Est, A., Bittl, R., Zech, S., Stehlik, D., Goldbeck, J. H., and Bryant, D. A. (2002) *Biochemistry* **41,** 394–405
11. Schultz, G., Ellerbrock, B. H., and Soll, J. (1981) *Eur. J. Biochem.* **117,** 329–332
12. Gaudillière, J.-P., d'Harlingue, A., Camara, B., and Monéger, R. (1984) *Plant Cell Rep.* **3,** 240–242
13. Seeger, J. W., Jr., and Bentley, R. (1991) *Phytochemistry* **39,** 3585–3589
14. Simantiras, M., and Leistner, E. (1991) *Z. Naturforsch.* **46c,** 364–370
15. Shimada, H., Ohno, R., Shibata, M., Ikegami, I., Onai, K., Ohto, M.-a., and Takamiya, K.-i. (2005) *Plant J.* **41,** 627–637
16. Gross, J., Cho, W. K., Lezhneva, L., Falk, J., Krupinska, K., Shinozaki, K., Seki, M., Herrmann, R. G., and Meurer, J. (2006) *J. Biol. Chem.* **281,** 17189–17196
17. Williams, J. G. K. (1988) *Methods Enzymol.* **167,** 766–778
18. Sattler, S. E., Cahoon, E. B., Coughlan, S. J., and DellaPenna, D. (2003) *Plant Physiol.* **132,** 2184–2195
19. Collakova, E., and DellaPenna, D. (2001) *Plant Physiol.* **127,** 1113–1124
20. Jakob, E., and Elmadfa, I. (1996) *Food Chemistry* **56,** 87–91
21. Bauer, J., Hiltbrunner, A., Weibel, P., Vidi, P. A., Alvarez-Huerta, M., Smith, M. D., Schnell, D. J., and Kessler, F. (2002) *J. Cell Biol.* **159,** 845–854
22. Murashige, T., and Skoog, F. (1962) *Physiol. Plant* **15,** 473–497
23. Rosso, M. G., Li, Y., Strizhov, N., Reiss, B., Dekker, K. A., and Weisshaar, B. (2003) *Plant Mol. Biol.* **53,** 247–259
24. Höfgen, R., and Willmitzer, L. (1990) *Plant Sci.* **66,** 221–230
25. Bent, A. F., Kunkel, B. N., Dahlbeck, D., Brown, K. L., Schmidt, R., Giraudat, J., Leung, J., and Staskawicz, B. J. (1994) *Science* **265,** 1856–1860
26. Sambrook, J., Fritsch, E., and Maniatis, T. (1989) *Molecular Cloning: A Laboratory Manual*, Ed. 2. Cold Spring Harbor Laboratory Press, Cold Spring Harbor, NY
27. Ischebeck, T., Zbierzak, A. M., Kanwischer, M., and Dörmann, P. (2006) *J. Biol. Chem.* **281,** 2470–2477
28. Porra, R. J., Thompson, W. A., and Kriedemann, P. E. (1989) *Biochim. Biophys. Acta* **975,** 384–394
29. Thayer, S. S., and Björkman, O. (1990) *Photosynth. Res.* **23,** 331–343
30. Noh, B., and Spalding, E. P. (1998) *Plant Physiol.* **116,** 503–509
31. Thompson, J. N., and Hatina, G. (1979) *J. Liquid Chromatogr.* **2,** 327–344

32. Vidi P.-A., Kanwischer M., Baginsky S., Austin J. R., Csucs G., Dörmann P., Kessler F., and Bréhélin C. (2006) *J. Biol. Chem.* **281,** 11225–11234

33. Browse, J., McCourt, P. J., and Somerville, C. R. (1986) *Anal. Biochem.* **152,** 141–145

34. Kirchhoff, H., Schöttler, M. A., Maurer, J., and Weis, E. (2004) *Biochim. Biophys. Acta* **1659,** 63–72

35. Scheller, H. V., and Haldrup, A. (2005) *Planta* **221,** 5–8

36. Schöttler, M. A., Kirchhoff, H., and Weis, E. (2004) *Plant Physiol.* **136,** 4265–4274

37. Lamkemeyer, P., Laxa, M., Collin, V., Li, W., Finkemeyer, I., Schöttler, M. A., Holtkamp, V., Tognetti, V. B., Issakidis-Bourguet, E., Kandlbinder, A., Weis, E., Miginiac-Maslow, M., and Dietz, K. J. (2006) *Plant J.* **45,** 968–981

38. Izawa, S. (2000) *Methods Enzymol.* **69,** 413–433

39. Schreiber, U., Schliwa, U., and Bilger, W. (1986) *Photosynth. Res.* **10,** 51–62

40. Lange, B. M., and Ghassemian M. (2003) *Plant Mol. Biol.* **51,** 925–948

41. Emanuelsson, O., Nielsen, H., Brunak, S., and von Heijne, G. (2000) *J. Mol. Biol.* **300,** 1005–1016

42. Valentin, H. E., Lincoln, K., Moshiri, F., Jensen, P. K., Qi, Q., Venkatesh, T. V., Karunanandaa, B., Baszis, S. R., Norris, S. R., Savidge, B., Gruys, K. J., and Last, R. L. (2006) *Plant Cell* **18,** 212–224

43. Ohl, S., Hahlbrock, K., and Schäfer, E. (1989) *Planta* **177,** 228–236

44. Gould, K. E. (2004) *J. Biomed. Biotechnol.* **5,** 314–320

45. Tevini, M., and Steinmüller, D. (1985) *Planta* **163,** 91–96

46. Porfirova, S., Bergmüller, E., Tropf, S., Lemke, R., and Dörmann, P. (2002) *Proc. Natl. Acad. Sci. U. S. A.* **99,** 12495–12500

47. Havaux, H., Eymery, F., Porfirova, S., Rey, P., and Dörmann, P. (2005) *Plant Cell* **17,** 3451–3469

48. Giacomelli, L., Rudella, A., and van Wijk, K.J. (2006) *Plant Physiol.* **141,** 685–701

49. Solfanelli, C., Poggi, A., Loreti, E., Alpi A., and Perata P. (2006) *Plant Physiol.* **140,** 637–646

50. Hope, A.B. (2000) *Biochim. Biophys. Acta* **1456,** 5–26

51. Finazzi, G., Sommer, F., and Hippler, M. (2005) *Proc. Natl. Acad. Sci. U. S. A.* **102,** 7031–7036